ELSEVIER

Catalysis Today 82 (2003) 241–254

CATALYSIS TODAY

www.elsevier.com/locate/cattod

Modeling a dense polymeric catalytic membrane reactor with plug flow pattern

José M. Sousa [a,b], Adélio Mendes [b,*]

[a] *Departamento de Química, Universidade de Trás-os-Montes e Alto Douro, Apartado 202, 5001-911 Vila-Real Codex, Portugal*
[b] *LEPAE—Departamento de Engenharia Química, Faculdade de Engenharia, Universidade do Porto, Rua Roberto Frias, 4200-465 Porto, Portugal*

Abstract

A theoretical study on a tubular membrane reactor assuming isothermal operation, plug flow pattern and using a dense polymeric catalytic membrane is performed. The reactor conversion for an equilibrium gas-phase reaction generically represented by A B is analyzed, considering the influence of the product's sorption and diffusion coefficients. It is concluded that the conversion of such a reaction can be significantly improved when the overall diffusion coefficient of the reaction product is higher than the reactant's one and/or the overall sorption coefficient is lower, and for Thiele modulus and contact time values over a threshold. Though a sorption coefficient of the reaction product lower than that of the reactant may leads to a conversion enhancement higher than that one obtained when the reaction product diffusion coefficient is higher than that of the reactant, the contact time value for the maximum conversion is much higher in the first case. In this way, a higher diffusion coefficient for the reaction product should be generally preferable, because it leads to a lower reactor size. The performance of a dense polymeric catalytic membrane reactor depends in a different way on both sorption and diffusion coefficients of reactants and products and then a study of such a system cannot be based only on their own permeabilities. Favorable combinations of diffusion and sorption coefficients can affect positively the reactor's conversion.
© 2003 Elsevier B.V. All rights reserved.

Keywords: Dense polymeric catalytic membrane; Plug flow reactor; Gas-phase reaction; Equilibrium reaction; Modeling

1. Introduction

The growing need for more environmentally safe and economically efficient processes has supplied the driving force for developing new technologies like the ones associated with the combined reaction–separation systems. Membrane reactors for chemical catalysis are in this new group of technologies and have attracted great interest since the pioneering work by Gryaznov et al. [1]. Most of the research has been focused on reactors with inorganic membranes, catalytic or not, mainly because of the usually high temperatures and, sometimes, the aggressive chemical environments. Some recent reviews summarize the state of the art in this area [2,3]. One of the most important objectives of the membrane reactor research has been to achieve a conversion enhancement over the thermodynamic equilibrium one based on the feed conditions, by selective removal of at least one reaction product from the reaction medium. The most studied class of reactions in this subject has been the hydrocarbon dehydrogenations [4–6].

Polymeric membranes cannot operate in such harsh conditions, so it is not surprising that they have hardly

* Corresponding author. Tel.: +351-22-5081695; fax: +351-22-5081449.
E-mail address: mendes@fe.up.pt (A. Mendes).

0920-5861/$ – see front matter © 2003 Elsevier B.V. All rights reserved.
doi:10.1016/S0920-5861(03)00239-6

Nomenclature

D_i	diffusion coefficient of component i (m^2/s)
D_{ref}	diffusion coefficient of the reference component (component A) (m^2/s)
H_i	Henry's sorption coefficient of component i ($mol/(m^3\,Pa)$)
H_{ref}	Henry's sorption coefficient of the reference component (component A) ($mol/(m^3\,Pa)$)
k_d	direct reaction rate constant (s^{-1})
K_e	reaction equilibrium constant
L	reactor's length (m)
p_i	partial pressure of species i in equilibrium with the sorbed concentration (Pa)
p_i^F	partial pressure of component i in the feed stream (Pa)
p_i^P	partial pressure of component i in the permeate stream (Pa)
p_i^R	partial pressure of component i in the retentate stream (Pa)
P_{ref}	reference pressure (feed pressure) (Pa)
P^P	total pressure in the permeate side (Pa)
P^R	total pressure in the retentate side (Pa)
Q^P	total permeate volumetric flowrate (m^3/s)
Q^R	total retentate volumetric flowrate (m^3/s)
Q_{ref}	reference volumetric flowrate (feed flowrate) (m^3/s)
r	membrane radial coordinate (m)
r^s	external membrane radius (shell side) (m)
r^t	internal membrane radius (tube side) (m)
R	universal gas constant ($Pa\,m^3/(mol\,K)$)
T	absolute temperature (K)
X_A	reactor conversion of reactant A
X_A^E	thermodynamic equilibrium conversion of reactant A, based on the feed conditions
z	tube/shell axial coordinate (m)

Greek symbols

α_i	dimensionless diffusion coefficient of component i
γ_i	dimensionless sorption coefficient of component i
Γ	dimensionless contact time
Γ_{MC}	dimensionless contact time at the maximum conversion
Γ_{TPC}	dimensionless contact time at the total permeation condition
δ	membrane thickness (m)
ζ^P	dimensionless total permeate volumetric flowrate
ζ^R	dimensionless total retentate volumetric flowrate
Θ	relative reaction coefficient
λ	dimensionless axial coordinate
ν_i	stoichiometric coefficient of component i ($\nu_A = -1$, $\nu_B = 1$)
ρ	dimensionless membrane spatial coordinate
Φ	Thiele modulus
χ_A	relative conversion (X_A/X_A^E)
Ψ_i	dimensionless partial pressure of species i in equilibrium with the sorbed concentration
Ψ^P	dimensionless total pressure in the permeate side
Ψ^R	dimensionless total pressure in the retentate side
Ψ_i^F	dimensionless partial pressure of component i in the feed
Ψ_i^P	dimensionless partial pressure of component i in the permeate stream
Ψ_i^R	dimensionless partial pressure of component i in the retentate stream

ever been used but in biocatalysis. However, they have attracted an increasing interest in the last years, as these materials present some advantages over inorganic membranes: their thickness can be easily controlled, large scale preparation is not a problem, they are easier to make free of defects and the cost of production is lower [7–9]. Besides, polymeric membranes are not as brittle as the ceramic ones; they can be easily fabricated in a number of forms (flat, tubes, tubules, hollow fibers, spiral wound) [2,10,11] and can be easily produced with incorporated catalysts (nanosized dispersed metallic clusters [12,13], zeolites and activated carbons [14] or metallic complexes [11,15,16]). As a consequence of these developments, there is a growing need for effective theoretical models that can help understanding the potentialities and the limitations of these reactors, leading to optimized designs.

Among the several studies in the open literature that deal with modeling of membrane reactors, only a few actually consider catalytic membranes (where the catalyst is either the membrane itself, is incorporated in the porous membrane structure/membrane surface, or is occluded inside a dense membrane) [17–23]. At the best of our knowledge and beyond our recent work [19,20], only a few researchers [17,21,23] modeled a dense polymeric catalytic membrane reactor, however, for conducting a liquid-phase reaction.

In a recent theoretical study, we analyzed the performance of a dense polymeric catalytic membrane reactor when running an equilibrium gas-phase reaction [19,20]. Such model assumes perfectly mixed flow pattern in both retentate and permeate sides, flat membrane and isothermal operation. Following the same strategy, we will consider in the present work a tubular membrane reactor with plug flow pattern in both retentate and permeate sides, operating in co-current mode and fed by the tube side. We chose a hypothetical equilibrium reaction A $\rightleftarrows$ B, where A and B can comprehend more than one reactant/product, because the proposed model has an analytical solution for the membrane mass balance equations, thus allowing for a more accurate and faster solution of the global model, although without compromising the main conclusions.

This study resulted from the work by Detlev Fritsch after he had successfully synthesized a dense polymeric membrane with nanoclusters of palladium homogeneously dispersed throughout it [12]. This new catalytic membrane could be produced as a composite one, with a porous support, which imparts the mechanical resistance to it. Several flow patterns could be proposed for describing the hypothetical membrane module of cylindrical shape membranes. The most simple model for describing both the retentate and permeate flow patterns is the plug flow. It also can be considered a cross-flow arrangement with plug flow pattern in the retentate side, probably better suited to describe a system of composite membranes. However, the aim of the present paper is to make a qualitative analysis using plug flow pattern as opposed to the already published perfectly mixed flow pattern [19,20]. Indeed the plug flow plus cross-flow pattern does not produce qualitatively different results from the ones obtained here [24].

2. Model development

Fig. 1 represents a sketch of the shell and tube type catalytic membrane reactor considered in the present study. The tube side (retentate) and shell side (permeate) are at different, but constant, total pressures P^{R} and P^{P}, respectively, and separated by a cylindrical membrane of thickness δ filled with a hypothetical nanosized catalyst homogeneously distributed throughout it. A reaction of the type A $\rightleftarrows$ B is considered. The proposed model for this reactor is based on the following main assumptions:

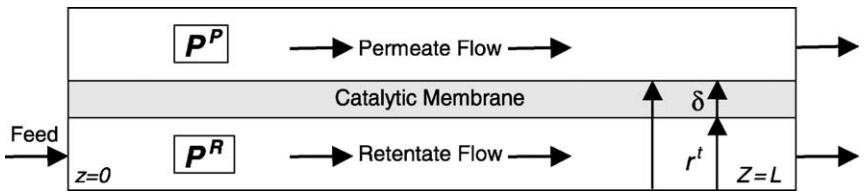

Fig. 1. Schematic diagram of the dense polymeric catalytic tubular membrane reactor (for co-current flow and tube side feed).

1. Steady state and isothermal operation.
2. Negligible film transport resistance in the membrane interface [25].
3. Plug flow pattern in both tube and shell sides.
4. Co-current operation and tube side feed.
5. Negligible pressure drop along the retentate and permeate sides.
6. Fickian transport through the membrane.
7. Sorption equilibrium between the bulk gas phase and the membrane surface described by the Henry's law.
8. Constant diffusion and sorption coefficients.
9. Elementary reaction mechanism.
10. Homogeneous catalyst distribution through the membrane [12].
11. The reaction occurs only on the catalyst surface.
12. Equal concentration on the catalyst surface and in the polymer matrix (any relationship could be considered in principle, but this one simplifies the original problem without compromising the main conclusions).

The mathematical model comprises the steady-state mass balances for the membrane, the retentate and the permeate sides, and the respective boundary conditions. In dimensionless form, the equations are as follows [24].

2.1. Partial and total mass balances in the retentate side

$$\frac{\mathrm{d}(\zeta^{\mathrm{R}}\Psi_i^{\mathrm{R}})}{\mathrm{d}\lambda} - \Gamma\,\alpha_i\gamma_i\left.\frac{\mathrm{d}\Psi_i}{\mathrm{d}\rho}\right|_{\rho=0,\lambda} = 0, \quad i = \mathrm{A,B} \tag{1}$$

$$\Psi^{\mathrm{R}}\frac{\mathrm{d}\zeta^{\mathrm{R}}}{\mathrm{d}\lambda} - \Gamma\sum_i \alpha_i\gamma_i\left.\frac{\mathrm{d}\Psi_i}{\mathrm{d}\rho}\right|_{\rho=0,\lambda} = 0, \quad i = \mathrm{A,B} \tag{2}$$

The respective boundary conditions are as follows: $\lambda = 0$, $\Psi_i^{\mathrm{R}} = \Psi_i^{\mathrm{F}}$ and $\zeta^{\mathrm{R}} = 1$.

2.2. Partial and total mass balances in the permeate side

$$\frac{\mathrm{d}(\zeta^{\mathrm{P}}\Psi_i^{\mathrm{P}})}{\mathrm{d}\lambda} + \left(1+\frac{\delta}{r^{\mathrm{t}}}\right)\Gamma\,\alpha_i\gamma_i\left.\frac{\mathrm{d}\Psi_i}{\mathrm{d}\rho}\right|_{\rho=1,\lambda} = 0,$$
$$i = \mathrm{A,B} \tag{3}$$

$$\Psi^{\mathrm{P}}\frac{\mathrm{d}\zeta^{\mathrm{P}}}{\mathrm{d}\lambda} + \left(1+\frac{\delta}{r^{\mathrm{t}}}\right)\Gamma\sum_i \alpha_i\gamma_i\left.\frac{\mathrm{d}\Psi_i}{\mathrm{d}\rho}\right|_{\rho=1,\lambda} = 0,$$
$$i = \mathrm{A,B} \tag{4}$$

The respective boundary conditions are: $\lambda = 1$, $\mathrm{d}\Psi_i^{\mathrm{P}}/\mathrm{d}\lambda = 0$ and $\lambda = 0$, $\zeta^{\mathrm{P}} = 0$.

2.3. Mass balance in the membrane

$$\frac{\mathrm{d}^2\Psi_i}{\mathrm{d}\rho^2} + \frac{1}{\rho + r^{\mathrm{t}}/\delta}\frac{\mathrm{d}\Psi_i}{\mathrm{d}\rho} + \nu_i\frac{\Phi^2}{\alpha_i\gamma_i}\left(\gamma_{\mathrm{A}}\Psi_{\mathrm{A}} - \frac{\gamma_{\mathrm{B}}\Psi_{\mathrm{B}}}{K_{\mathrm{e}}}\right) = 0, \quad i = \mathrm{A,B} \tag{5}$$

The boundary conditions for Eq. (5) are the following:

$$\rho = 0\,(\forall\lambda), \quad \Psi_i = \Psi_i^{\mathrm{R}}(\lambda) \quad \text{and} \quad \rho = 1\,(\forall\lambda), \quad \Psi_i = \Psi_i^{\mathrm{P}}(\lambda)$$

The analytical solution of Eq. (5) is [24]

$$\begin{bmatrix}\Psi_{\mathrm{A}}\\ \Psi_{\mathrm{B}}\end{bmatrix} = (C_1 + C_2\ln\sigma)\begin{bmatrix}1\\ \dfrac{K_{\mathrm{e}}}{\gamma_{\mathrm{B}}}\end{bmatrix} + C_3\begin{bmatrix}1\\ -\dfrac{1}{\alpha_{\mathrm{B}}\gamma_{\mathrm{B}}}\end{bmatrix} \times I_0(\omega) + C_4\begin{bmatrix}1\\ -\dfrac{1}{\alpha_{\mathrm{B}}\gamma_{\mathrm{B}}}\end{bmatrix}K_0(\omega) \tag{6}$$

and

$$\Psi^{\mathrm{R}} = \frac{P^{\mathrm{R}}}{P_{\mathrm{ref}}}, \quad \Psi_i^{\mathrm{R}} = \frac{p_i^{\mathrm{R}}}{P_{\mathrm{ref}}}, \quad \Psi^{\mathrm{P}} = \frac{P^{\mathrm{P}}}{P_{\mathrm{ref}}}, \quad \Psi_i^{\mathrm{P}} = \frac{p_i^{\mathrm{P}}}{P_{\mathrm{ref}}}, \quad \Psi_i^{\mathrm{f}} = \frac{p_i^{\mathrm{f}}}{P_{\mathrm{ref}}}, \quad \Psi_i = \frac{p_i}{P_{\mathrm{ref}}}$$

$$\zeta^{\mathrm{R}} = \frac{Q^{\mathrm{R}}}{Q_{\mathrm{ref}}}, \quad \zeta^{\mathrm{P}} = \frac{Q^{\mathrm{P}}}{Q_{\mathrm{ref}}}, \quad \rho = \frac{r - r^{\mathrm{t}}}{\delta}, \quad \lambda = \frac{z}{L}, \quad \alpha_i = \frac{D_i}{D_{\mathrm{ref}}}, \quad \gamma_i = \frac{H_i}{H_{\mathrm{ref}}}$$

$$\Phi = \delta\left(\frac{k_{\mathrm{d}}}{D_{\mathrm{ref}}}\right)^{1/2}, \quad \sigma = \rho + \frac{r^{\mathrm{t}}}{\delta},$$
$$\Gamma = \frac{2\pi r^{\mathrm{t}} L D_{\mathrm{ref}} H_{\mathrm{ref}} RT}{\delta Q_{\mathrm{ref}}},$$
$$\omega^2 = \Phi^2\left(1 + \frac{1}{\alpha_{\mathrm{B}}K_{\mathrm{e}}}\right)\left(\rho + \frac{r^{\mathrm{t}}}{\delta}\right)^2$$

$$C_1 = \frac{(\Psi_A^P(\lambda) + \alpha_B\gamma_B\Psi_B^P(\lambda))\ln(\delta/r^t) + (\Psi_A^R(\lambda) + \alpha_B\gamma_B\Psi_B^R(\lambda))\ln(1 + r^t/\delta)}{(1 + \alpha_B K_e)\ln(1 + \delta/r^t)}$$

$$C_2 = \frac{\Psi_A^P(\lambda) - \Psi_A^R(\lambda) + \alpha_B\gamma_B(\Psi_B^P(\lambda) - \Psi_B^R(\lambda))}{(1 + \alpha_B K_e)\ln(1 + \delta/r^t)}$$

$$C_3 = \frac{(\alpha_B K_e\Psi_A^R(\lambda) - \alpha_B\gamma_B\Psi_B^R(\lambda))K_0(\eta(1 + \delta/r^t)) - (\alpha_B K_e\Psi_A^P(\lambda) - \alpha_B\gamma_B\Psi_B^P(\lambda))K_0(\eta\delta/r^t)}{(1 + \alpha_B K_e)[I_0(\eta\delta/r^t)K_0(\eta(1 + \delta/r^t)) - I_0(\eta(1 + \delta/r^t))K_0(\eta\delta/r^t)]}$$

$$C_4 = -\frac{(\alpha_B K_e\Psi_A^R(\lambda) - \alpha_B\gamma_B\Psi_B^R(\lambda))I_0(\eta(1 + \delta/r^t)) - (\alpha_B K_e\Psi_A^P(\lambda) - \alpha_B\gamma_B\Psi_B^P(\lambda))I_0(\eta\delta/r^t)}{(1 + \alpha_B K_e)[I_0(\eta\delta/r^t)K_0(\eta(1 + \delta/r^t)) - I_0(\eta(1 + \delta/r^t))K_0(\eta\delta/r^t)]}$$

The subscripts i and ref refer to the ith and reference components and the superscripts F, R and P refer to the feed, retentate and permeate streams, respectively. Φ represents the Thiele modulus (ratio between the characteristic diffusion time of the reference component and the characteristic reaction time of the direct reaction) and Γ represents the dimensionless contact time (ratio between the characteristic feed flow time and the characteristic permeation time of the reference component). Feed conditions are taken as the reference for P_{ref} and Q_{ref}. Component A is taken as the reference for D_{ref} and H_{ref}. $I_0(\omega)$ and $K_0(\omega)$ are the modified Bessel functions of order 0. The other symbols are referred in nomenclature.

The membrane reactor performance is evaluated from the results of the relative conversion, χ_A, which is defined as the ratio between the reactor's conversion of reactant A, X_A, and the thermodynamic equilibrium conversion based on feed conditions, X_A^E. The reactor's conversion is calculated using the conventional equation:

$$X_A = 1 - \frac{\zeta^R\Psi_A^R + \zeta^P\Psi_A^P}{\zeta^F\Psi_A^F} \quad (7)$$

We still need to define the relative reaction coefficient, which measures how the reactive system is far from the thermodynamic equilibrium:

$$\Theta = \frac{\gamma_B\Psi_B/\gamma_A\Psi_A}{K_e} \quad (8)$$

2.4. Solution strategy

The general strategy used for solving the model equations is the same as adopted before [19,20]: in order to overcome numerical instability problems, a time derivative term was added to the right-hand side of Eqs. (1) and (3), transforming this problem into a pseudo-transient one. The mass balance equations in the membrane were solved analytically; ζ^R and ζ^P were calculated by the integration of Eqs. (2) and (4) using Simpson's rule. The partial differential equations resulting from (1) and (3) were spatially discretized using a tailor made code based on finite differences. The time integration routine LSODA [26] was then used to integrate the resulting set of time dependent equations. The solution is considered to be in steady state when the time derivative of each dependent variable and for each of the spatial coordinate is smaller than a pre-defined value.

3. Results and discussion

With the present study, we want to understand theoretically how the relative conversion depends on the contact time (Γ) and Thiele modulus (Φ) for different sets of diffusion and sorption coefficients of the reaction components. Firstly, we consider a base case, where all dimensionless diffusion and sorption coefficients are equal to the unity. Afterwards, some combinations of component B dimensionless diffusion or sorption coefficients are studied, so that its permeability becomes smaller or larger than one, keeping component A parameters' as in the base case. We should remember that the membrane permeability towards a component i is the product of its diffusion and sorption coefficients, $L_i = D_i H_i$; or, in its dimensionless form, $\Pi_i = \alpha_i\gamma_i$, where $\Pi_i = L_i/L_A$.

It should be highlighted that it is the ability of the membrane to allow a selective mass transport for reactants and products that makes possible an enhancement of the relative conversion above unity (i.e. a reactor's

conversion higher than the thermodynamic value for the same conditions). In this way, the meaning of the already defined Thiele modulus in the framework of catalytic membrane reactors should not be considered the same as it is in the framework of conventional packed bed reactors: here, it simply represents a ratio between the characteristic time for the direct reaction and the characteristic time for the diffusion of the reference component.

3.1. Base case—equal permeability for all reaction components ($\alpha_i = 1$; $\gamma_i = 1$)

Fig. 2 shows the relative conversion of the reactor as a function of the contact time for various Thiele moduli. Since all components have the same diffusion and sorption coefficients (there is no separation effect) and $\sum \nu_i = 0$, the maximum achievable conversion should be the thermodynamic equilibrium value for the feed conditions.

For a given Thiele modulus value, the relative conversion increases with contact time up to an end point where the retentate flowrate leaving the reactor is zero, i.e. all the species permeate through the membrane. This condition is called total permeation condition (TPC) or 100% cut. The curves of relative conversion for different Thiele moduli have an end point corresponding to the TPC; the locus of these end points is defined as total permeation line (TPL).

For a specified Thiele modulus value, the relative conversion increases monotonically with contact time only because the relative flowrate that contact with the catalyst (permeates through the membrane) increases continuously. Nevertheless, we may distinguish two different operation zones, depending on the Thiele modulus. For low Thiele modulus values (Φ lower about 2.5 in the present case), the relative conversion is always smaller than 1, because the characteristic reaction time is higher than the characteristic diffusion time. As a result, a fraction of the reactant crosses the membrane without reacting and the relative reaction coefficient (see Eq. (8)) is always lower than 1. We could call this regime as chemical regime. For Thiele modulus values higher than about 2.5, the reactor operates in what we may call diffusional regime. Depending on the Thiele modulus value, the chemical reaction reaches the thermodynamic equilibrium inside the membrane, starting somewhere quite close to the permeate side (radial position) and for an axial coordinate close to the exit of the reactor. As the Thiele modulus increases, the chemical equilibrium condition is progressively extended along the membrane

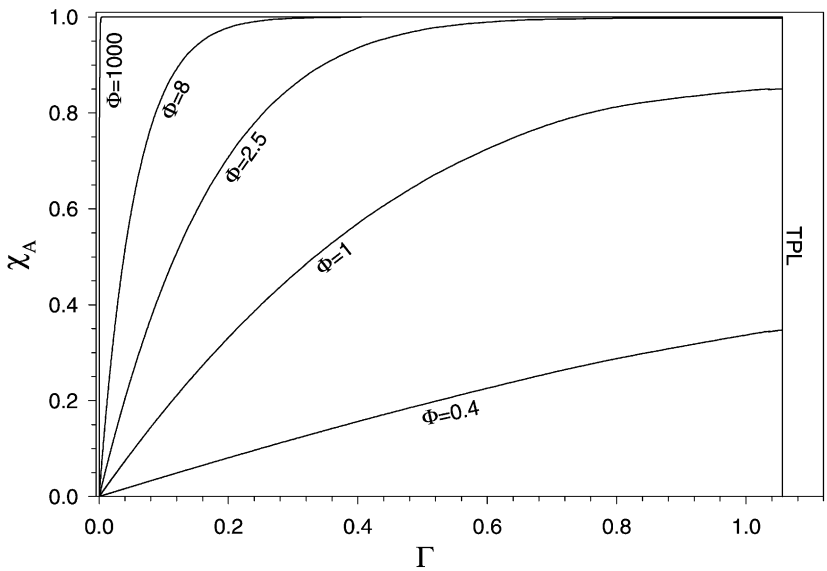

Fig. 2. Relative conversion as a function of the contact time for different Thiele modulus values ($\alpha_i = 1$, $\gamma_i = 1$, $\Psi_A^F = 1$, $\Psi^R = 1$, $\Psi^P = 0.1$, $r^t/\delta = 10$ and $K_e = 0.25$).

thickness. Eventually, the maximum conversion is attained, depending on both the contact time and the Thiele modulus values. For an instantaneous reaction ($\Phi \rightarrow \infty$), the reaction will be in chemical equilibrium through all the membrane and the attained conversion will be equal to the thermodynamic one, independently of the contact time value. As all the components have the same permeability, the contact time for the total permeation condition is constant.

3.2. Permeability of component B higher than permeability of component A ($\Pi_B > 1$)

In this section, we consider two different situations where the permeability of component B is higher than that of component A: higher diffusion coefficient of reaction product with equal sorption coefficients for all components and higher sorption coefficient of reaction product with equal diffusion coefficients for all components.

Fig. 3 shows the relative conversion of the reactor as a function of the contact time and for different Thiele modulus values, for a dimensionless diffusion coefficient of component B higher than 1, $\alpha_B = 10$, and keeping all the other relevant variables as in the base case. It is clear from these results that, for a given system and for a set of operation conditions, the attainable conversion in the reactor could be far above the thermodynamic equilibrium one. The reason for this enhancement is the preferential diffusion of the reaction product through the membrane, thus shifting the chemical reaction towards the products side beyond the equilibrium value; from this point on, we will call this behavior as *separation effect*. As in the base case, the maximum conversion is attained at the total permeation condition and for the same reason: the catalyst usage is maximized, i.e. all the reactants must permeate through the membrane.

Another conclusion from this figure is that, depending on the Thiele modulus, the separation effect leads to two different behaviors in the evolution of the reactor conversion. For low Thiele modulus values, the reactor operates in chemical regime. So, an increasing of the conversion with the Thiele modulus is expected, as the catalyst is more and more effectively used (see Fig. 4). As the Thiele modulus value increases, the reaction coefficient is getting closer and closer the equilibrium constant ($\Theta \rightarrow 1$) and, due to the separation effect, even surpass this value ($\Theta > 1$) in a final fraction of the membrane thickness on the permeate side. For this chemical regime operation, the molar fraction of the reaction product at the exit of the reactor

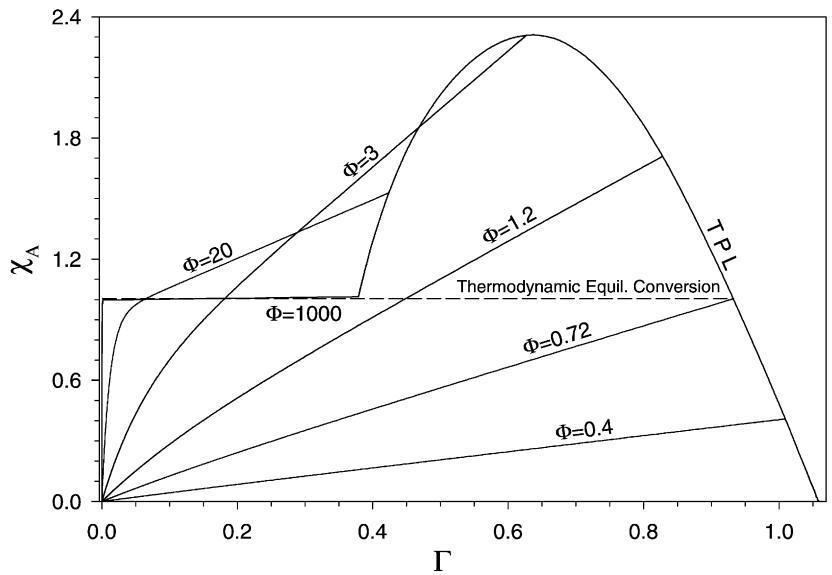

Fig. 3. Relative conversion as a function of the contact time for different Thiele modulus values ($\alpha_A = 1$, $\alpha_B = 10$, $\gamma_i = 1$, $\Psi_A^F = 1$, $\Psi^R = 1$, $\Psi^P = 0.1$, $r^t/\delta = 10$ and $K_e = 0.25$).

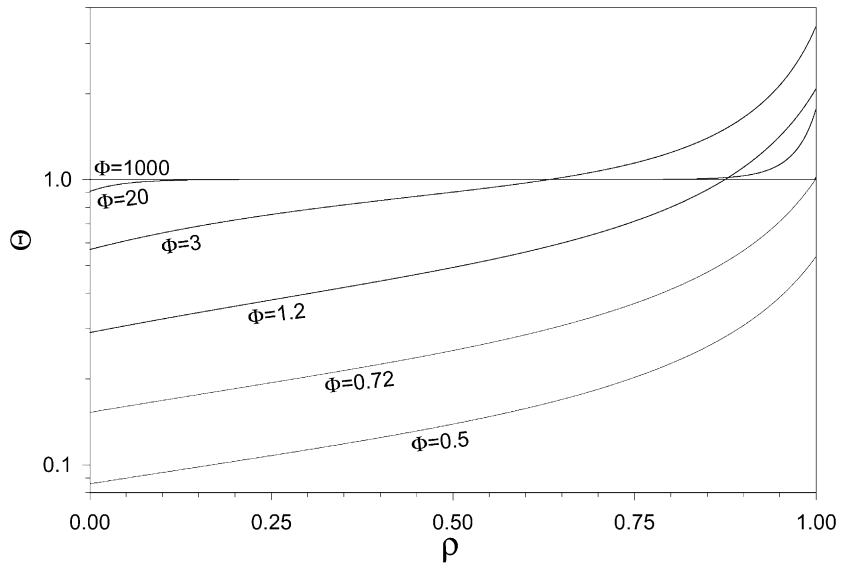

Fig. 4. Relative reaction coefficient as a function of the membrane's radial coordinate for various Thiele modulus values ($\alpha_A = 1$, $\alpha_B = 10$, $\gamma_i = 1$, $\Psi_A^F = 1$, $\Psi^R = 1$, $\Psi^P = 0.1$, $r^t/\delta = 10$, $K_e = 0.25$, $\Gamma = \Gamma_{TPC}$ and $\lambda = 1$).

increases continuously with the Thiele modulus value, either on the retentate or on the permeate streams, leading to an increasing of the conversion (see Fig. 5).

As a consequence of the reaction coefficient overtaking the equilibrium constant, the backward reaction rate overlaps the direct reaction rate. For Thiele modulus values below a threshold value ($\Phi \cong 3$, in this case), this backward reaction effect is offset, because the characteristic diffusion time is shorter than the characteristic reaction time. For Thiele modulus values above about 3, the ratio between the characteristic diffusion and reaction times is inverted. As a result, the chemical reaction attains local equilibrium somewhere in an inward fraction of the catalytic membrane thickness. As the Thiele modulus value increases, the membrane fraction where the reaction is in equilibrium is enlarged and the equilibrium shift due to the preferential diffusion of the reaction product is more and more offset by the backward reaction. In this case, the reactor operates in diffusional regime and the result of this behavior can also be seen in Fig. 5. For the retentate side, the molar fraction of the reaction product increases continuously by means of the increase of the Thiele modulus, because the equilibrium front in the membrane is moving closer and closer to the membrane surface at the retentate side, increasing this way the driving force to withdraw the reaction product from the membrane. For the permeate side, on the other hand, the molar fraction of the same component decreases continuously, leading to a decrease in the conversion (see Fig. 5). For a high Thiele modulus value ($\Phi \to \infty$), the chemical reaction is in equilibrium through all the membrane. In this way, any separation effect is completely offset and the reactor conversion is equal to the thermodynamic equilibrium one, whichever is the contact time. We should still point out the fact that, though the results of Fig. 4 were obtained for the outlet of the reactor and at the total permeation condition, the same conclusions could be set for a lower contact time, as can be seen from Fig. 5. Indeed, concerning the evaluation of the results for an internal axial position of the reactor ($\lambda < 1$), they are equivalent to that we would get if we considered a lower contact time for $\lambda = 1$, as can be concluded from the definition of Γ.

It is worth noting that the contact time at the total permeation condition decreases with the Thiele modulus value until a limit value for high Thiele modulus values, although the reactor conversion does not follow the same trend (see Fig. 3). The decrease of the contact time with an increase of the conversion is expected, because the reaction transforms a slower

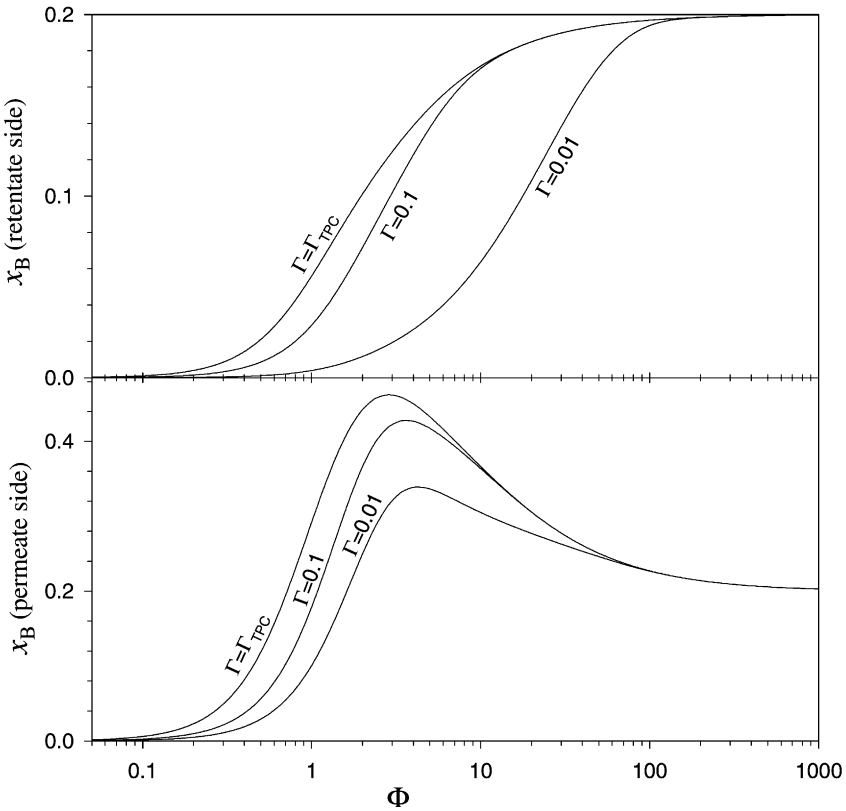

Fig. 5. Molar fraction of the component B in the retentate (upper part) and permeate (lower part) outlet streams as a function of the Thiele modulus and for different contact time values ($\alpha_A = 1$, $\alpha_B = 10$, $\gamma_i = 1$, $\Psi_A^F = 1$, $\Psi^R = 1$, $\Psi^P = 0.1$, $r^t/\delta = 10$, $\lambda = 1$ and $K_e = 0.25$).

component (reactant) in a faster one (reaction product). For the diffusional regime, on the other hand, the contact time at the total permeation condition reflects the balance of two opposite trends: decreasing the conversion increases the contact time and increasing the Thiele modulus value leads the locus inside the membrane where the chemical equilibrium is attained to move towards the membrane surfaces. For low *r*-values (retentate side) this shift reduces the path that the slowest component has to travel until the chemical equilibrium is reached. Let us consider, for example, the maximum conversion for $\Phi = 0.72$ and for $\Phi = 1000$, which is approximately equal to the thermodynamic equilibrium value (Fig. 3) and the respective relative reaction coefficient profile (Fig. 4). As can be seen, the mean residence time of both reaction components inside the membrane is much higher for $\Phi = 0.72$, because the higher relative concentration of component A inside the membrane. For high *r*-values (permeate side), the local equilibrium front moves towards the permeate side, leading to a conversion decrease and, consequently, to an increase of the contact time.

Fig. 6 shows the relative conversion of the reactor as a function of the contact time, for different Thiele modulus values, for dimensionless sorption coefficient of component B higher than 1, $\gamma_B = 10$, and keeping all the other relevant variables as for the base case. In this example, the maximum conversion attained in the reactor is much smaller than the thermodynamic equilibrium one. The high sorption affinity of the membrane towards reaction product keeps it in a high concentration inside the membrane while the concentration in the gas phase (retentate and permeate sides) is low, thus penalizing strongly the conversion. The similarity between Figs. 3 and 6 is to the same relative permeabilities for the reaction components.

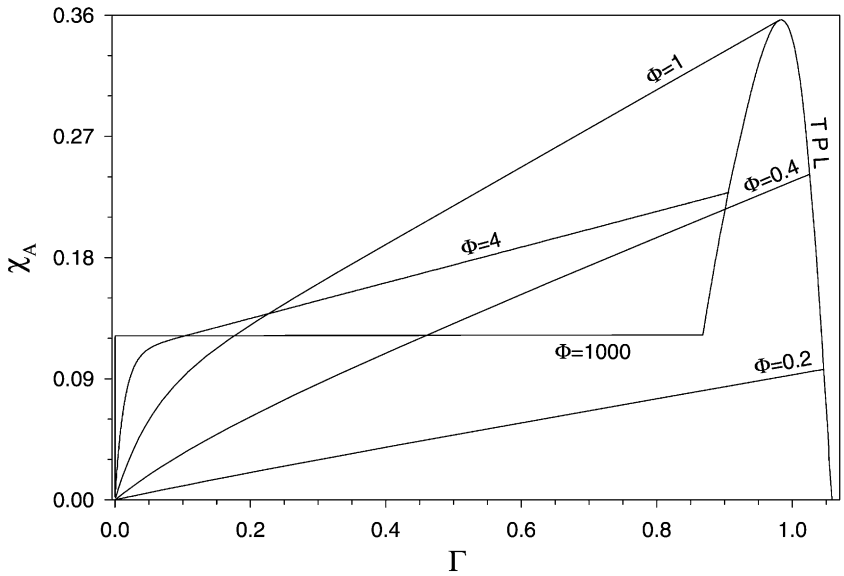

Fig. 6. Relative conversion as a function of the contact time for different Thiele modulus values ($\alpha_i = 1$, $\gamma_A = 1$, $\gamma_B = 10$, $\Psi_A^F = 1$, $\Psi^R = 1$, $\Psi^P = 0.1$, $r^t/\delta = 10$ and $K_e = 0.25$).

3.3. Permeability of component B lower than permeability of component A ($\Pi_B < 1$)

In this section we consider the case where the permeability of component B is smaller than that of component A. As in the previous example, we will focus solely on two different situations: lower diffusion coefficient of the reaction product with equal sorption coefficients for all components and lower sorption coefficient of the reaction product with equal diffusion coefficients for all components. Fig. 7 shows the relative conversion of the reactor as a function of the contact time and for different Thiele moduli, for a dimensionless sorption coefficient of component B lower than 1, $\gamma_B = 0.1$, and keeping all the other relevant variables as for the base case. As expected, the conversion attained in the reactor surpasses largely the thermodynamic equilibrium value. The low affinity of the membrane towards the reaction product keeps it in a low concentration inside the membrane, thus favoring the conversion. Nevertheless, the pattern of these results is completely different from the ones illustrated in Fig. 3 or Fig. 6. Firstly, the reactor's conversion for a given contact time value increases continuously with the Thiele modulus until the maximum conversion is attained for $\Phi \to \infty$. Secondly, the reactor conversion for a given Thiele modulus value increases as a function of the contact time until a maximum value and then decreases until the total permeation condition, for almost the whole Thiele moduli range.

For a given contact time value, the conversion increases continuously with the Thiele modulus up to its maximum value (for $\Phi \to \infty$) as a net result of the contributions from the retentate and permeate sides. The contribution from the permeate side is always positive, i.e. the conversion increases always with the Thiele modulus value (see Fig. 8). Because its higher permeability, component A tends to escape from the membrane faster than component B does, thus pulling down the reaction coefficient in a membrane fraction quite close to the permeate side. In this way, an increase in the Thiele modulus value results in a more effective use of the catalyst. On the other hand, there are some operation regions where the contribution of the retentate side is negative, i.e. the conversion decreases with the Thiele modulus after a turning point. This is also a result of the separation effect, which leads to a higher backward reaction rate than the direct reaction rate (see Fig. 8). However, this backward reaction effect only occurs for medium/high Thiele modulus values and contact times not far from the total permeation condition. The net balance between these two trends is

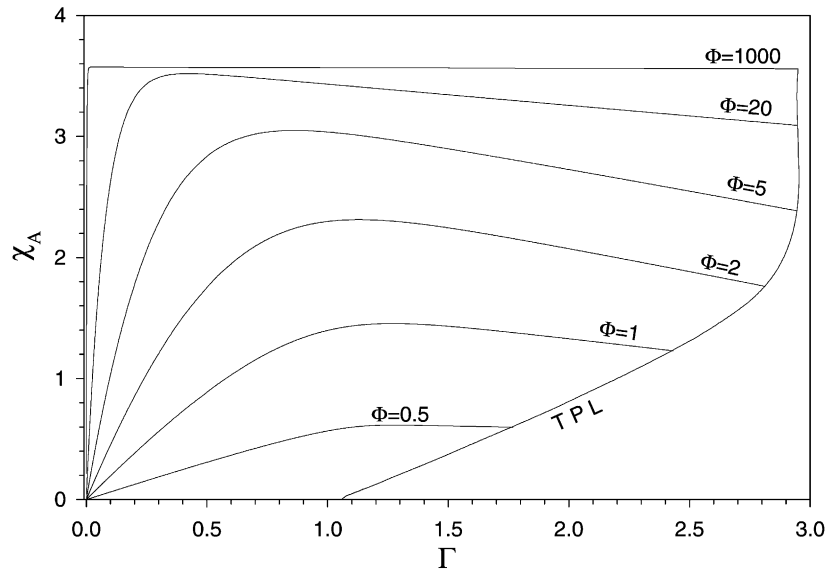

Fig. 7. Relative conversion as a function of the contact time for different Thiele modulus values ($\alpha_i = 1$, $\gamma_A = 1$, $\gamma_B = 0.1$, $\Psi_A^F = 1$, $\Psi^R = 1$, $\Psi^P = 0.1$, $r^t/\delta = 10$ and $K_e = 0.25$).

still positive with respect to the conversion, although its increase with the Thiele modulus slows down.

Contrary to the continuous increase of the conversion with the Thiele modulus for a given contact time, the evolution of the conversion as a function of the contact time, for a given Thiele modulus value, shows a maximum before the total permeation condition, for almost the whole Thiele moduli range (see Fig. 7).

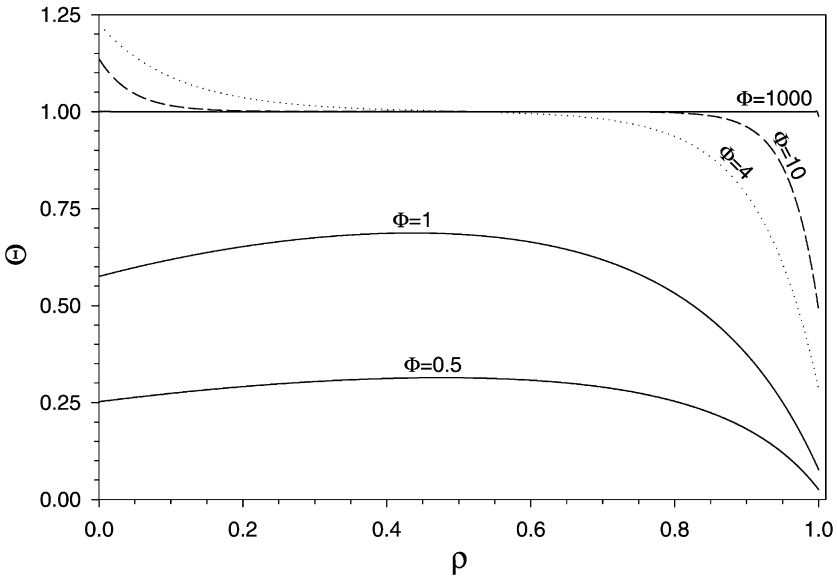

Fig. 8. Relative reaction coefficient as a function of the membrane's radial coordinate for various Thiele modulus values ($\alpha_i = 1$, $\gamma_A = 1$, $\gamma_B = 0.1$, $\Psi_A^F = 1$, $\Psi^R = 1$, $\Psi^P = 0.1$, $r^t/\delta = 10$, $K_e = 0.25$, $\Gamma = 1$ and $\lambda = 1$).

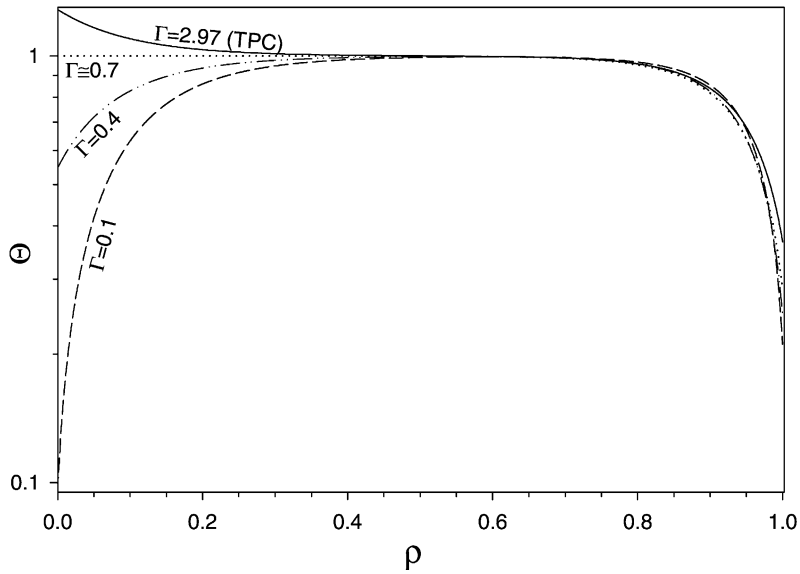

Fig. 9. Relative reaction coefficient as a function of the membrane's radial coordinate for various contact time values ($\alpha_i = 1$, $\gamma_A = 1$, $\gamma_B = 0.1$, $\Psi_A^F = 1$, $\Psi^R = 1$, $\Psi^P = 0.1$, $r^t/\delta = 10$, $\lambda = 1$, $\Phi = 5$ and $K_e = 0.25$).

Let us consider, for example, the evolution of the relative conversion for $\Phi = 5$, which displays a maximum of $\chi_A \cong 3.06$ set at $\Gamma \cong 0.9$, called henceforth Γ_{MC}. The concentration of component A as a function of the contact time tends to decrease quickly, due, in one hand, to the consumption by the chemical reaction and, on the other hand, to its higher permeability. For low contact times, component A concentration in

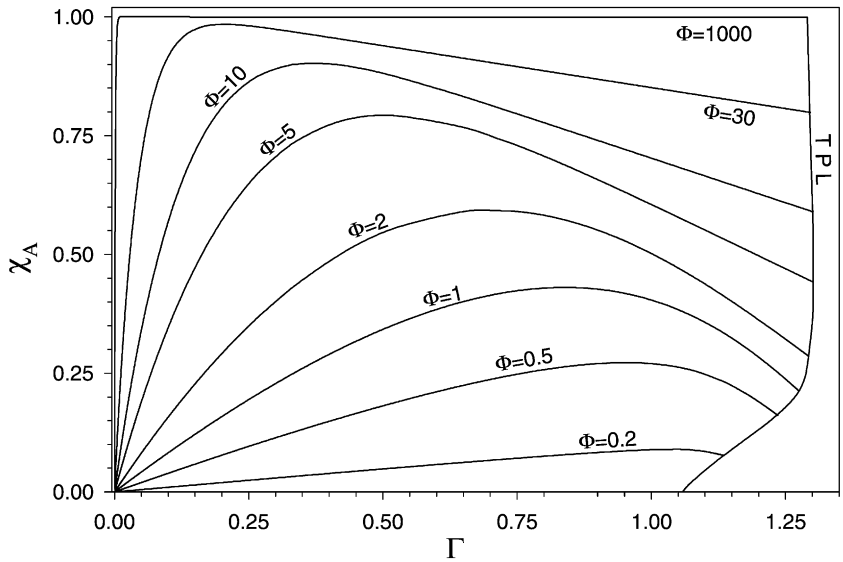

Fig. 10. Relative conversion as a function of the contact time for different Thiele modulus values ($\alpha_A = 1$, $\alpha_B = 0.1$, $\gamma_i = 1$, $\Psi_A^F = 1$, $\Psi^R = 1$, $\Psi^P = 0.1$, $r^t/\delta = 10$ and $K_e = 0.25$).

the retentate flow is high enough, as well as inside the membrane. In this way, the chemical reaction is always on or under the equilibrium condition (see Fig. 9). So, increasing the contact time, i.e. increasing the fraction of the feed that crosses the membrane, leads to a more effective use of the catalyst and the conversion increases quickly. As the contact time increases, component A is quickly depleted down to a minimum value and component B begins to be in excess with respect to the chemical equilibrium condition and then the reaction coefficient overtakes the chemical equilibrium constant (see Fig. 9). From this point on, the back reaction and the back diffusion of component B produced earlier on (i.e. for lower z values) keep the reaction components concentration approximately at a constant level. This behavior leads to the conversion decrease, despite the already referred favorable effect which occurs in the permeate side (the results showed in Fig. 9 refer to the reactor outlet, i.e. to $z = L$). As in Figs. 3 and 6, the evolution of the contact time at the total permeation condition is a net result of the conversion increase (which leads to an increase of the contact time) and the change of the average reaction components' residence time.

Fig. 10 shows the relative conversion of the reactor as a function of the contact time and for different Thiele moduli, for a dimensionless diffusion coefficient of component B lower than 1, $\alpha_B = 0.1$, and keeping all the other relevant variables as for the base case. It is worth to notice that the maximum conversion attained is the thermodynamic equilibrium one, for $\Phi \to \infty$. This happens because the separation effect is completely offset in such conditions and the affinity of the membrane for both reaction components is the same. Despite the same components' permeabilities, the conversion is strongly penalized.

4. Conclusions

In the present study, we analyzed a dense polymeric catalytic membrane reactor operating in isothermal conditions for co-current arrangement and plug flow. A study was made of the influence that the sorption and diffusion coefficients of reactants and products play in the conversion attained in this reactor. An equilibrium-limited gas-phase reaction of the type $A \rightleftarrows B$ was considered for the sole reason that an analytical solution of the mass balance equations for the membrane can be written. The obtained results showed that, for a given set of conditions, it is possible to obtain conversions well above the thermodynamic value. This is the case when the reaction products have a lower sorption coefficient and/or a higher diffusion coefficient than the reactants one. Nevertheless, it should be emphasized that a lower sorption coefficient of the reaction product leads to a much higher contact time value than a higher diffusion coefficient of the reaction product, despite the relatively higher attainable conversion (note that the reactor size is directly proportional to the contact time).

Acknowledgements

José R. Sousa acknowledges a grant from FCT to attend the ICCMR5 congress. The authors acknowledge the research project Sapiens 32452/99 funded by FCT. The authors also thank Dr. Peter Janknecht for his careful revision of the manuscript.

References

[1] V.M. Gryaznov, M.M. Ermilova, N.V. Orekhova, Membrane–catalyst systems for selectivity improvement in dehydrogenation and hydrogenation reactions, Catal. Today 67 (2001) 185.
[2] K.K. Sirkar, P.V. Shanbhag, A.S. Kovvali, Membrane in a reactor: a functional perspective, Ind. Eng. Chem. Res. 38 (1999) 3715.
[3] J. Zaman, A. Chakma, Inorganic membrane reactors—review, J. Membr. Sci. 92 (1994) 1.
[4] H. Weyten, J. Luyten, K. Keizer, L. Willems, R. Leysen, Membrane performance: the key issues for dehydrogenation reactions in a catalytic membrane reactor, Catal. Today 56 (2000) 3.
[5] J. Shu, B.P.A. Grandjean, A. van Neste, S. Kaliaguine, Catalytic palladium-based membrane reactors—a review, Can. J. Chem. Eng. 69 (1991) 1036.
[6] N. Itoh, T.-H. Wu, An adiabatic type of palladium membrane reactor for coupling endothermic and exothermic reactions, J. Membr. Sci. 124 (1997) 213.
[7] I.F.J. Vankelecom, K.A.L. Vercruysse, P.E. Neys, D.W.A. Tas, K.B.M. Janssen, P.-P. Knops-Gerrits, P.A. Jacobs, Novel catalytic membranes for selective reactions, Top. Catal. 5 (1998) 125.
[8] J. Sanchez, T.T. Tsotsis, Current developments and future research in catalytic membrane reactors, in: A.J. Burggraaf, L. Cot (Eds.), Fundamentals of Inorganic Science and Technology, Elsevier, Amsterdam, 1996, pp. 529–568.

[9] S. Tennison, Current hurdles in the commercial development of inorganic membrane reactor, in: Proceedings of the Fourth International Conference on Catalysis in Membrane Reactors, Zaragoza, Spain, 3–5 July 2000, pp. 13–17.
[10] W.J. Koros, R.T. Chern, Separation of gaseous mixtures using polymer membranes, in: R.W. Rousseau (Ed.), Handbook of Separation Process Technology, Wiley, 1987, pp. 862–953.
[11] I.F.J. Vankelecom, P.A. Jacobs, Dense organic catalytic membranes for fine chemical synthesis, Catal. Today 56 (2000) 147.
[12] D. Fritsch, K.-V. Peinemann, Novel highly permselective 6F-poly(amide–imide)s as membrane host for nano-sized catalysts, J. Membr. Sci. 99 (1995) 29.
[13] J.F. Ciebien, R.E. Cohen, A. Duran, Catalytic properties of palladium nanoclusters synthesized within diblock copolymer films: hydrogenation of ethylene and propylene, Supramol. Sci. 5 (1998) 31.
[14] J. Vital, A.M. Ramos, I.F. Silva, H. Valente, J.E. Castanheiro, Hydration of α-pinene over zeolites and activated carbons dispersed in polymeric membranes, Catal. Today 56 (2000) 167.
[15] P.E.F. Neys, A. Severeyns, I.F.J. Vankelecom, E. Ceulemans, W. Dehaen, P.A. Jacobs, Manganese porphyrins incorporated in PDMS: selective catalysts for the epoxidation of deactivated alkenes, J. Mol. Catal. 144 (1999) 373.
[16] G. Langhendries, G.V. Baron, I.F.J. Vankelecom, R.F. Parton, P.A. Jacobs, Selective hydrocarbon oxidation using a liquid-phase catalytic membrane reactor, Catal. Today 56 (2000) 131.
[17] A.A. Yawalker, V.G. Pangarkar, G.V. Baron, Alkene epoxidation with peroxide in a catalytic membrane reactor: a theoretical study, J. Membr. Sci. 182 (2001) 129.
[18] H.W.J.P. Neomagus, G. Saracco, H.F.W. Wessel, F. Versteeg, The catalytic combustion of natural gas in a membrane reactor with separate feed of reactants, Chem. Eng. J. 77 (2000) 165.
[19] J.M. Sousa, P. Cruz, A. Mendes, Modeling a catalytic polymeric non-porous membrane reactor, J. Membr. Sci. 181 (2001) 241.
[20] J.M. Sousa, P. Cruz, A. Mendes, A study on the performance of a dense polymeric catalytic membrane reactor, Catal. Today 67 (2001) 281.
[21] J. Vital, A.M. Ramos, I.F. Silva, H. Valente, J.E. Castanheiro, The effect of α-terpineol on the hydration of α-pinene over zeolites dispersed in polymeric membranes, Catal. Today 67 (2001) 217.
[22] M.P. Harold, C. Lee, Intermediate product yield enhancement with a catalytic inorganic membrane. II. Nonisothermal and integral operation in a back-mixed reactor, Chem. Eng. Sci. 52 (1997) 1923.
[23] S. Wu, J.-E. Gallot, M. Bousmina, C. Bouchard, S. Kaliaguine, Zeolite containing catalytic membranes as interphase contactors, Catal. Today 56 (2000) 113.
[24] J.M. Sousa, A. Mendes, Simulation study of a dense polymeric catalytic membrane reactor with plug flow pattern, Chem. Eng. J., in press.
[25] M. Mulder, Basic Principles of Membrane Technology, Kluwer Academic Publishers, Dordrecht, The Netherlands, 2000.
[26] L.R. Petzold, A.C. Hindmarsh, LSODA, Computing and Mathematics Research Division, Lawrence Livermore National Laboratory, 1997.